

Genetic Influence underlying Brain Connectivity Phenotype: A Study on Two Age-Specific Cohorts

Shan Cong¹, Xiaohui Yao¹, Linhui Xie², Jingwen Yan³, Li Shen^{1*}

¹Perelman School of Medicine, University of Pennsylvania, United States, ²Purdue School of Engineering and Technology, Indiana University, Purdue University Indianapolis, United States, ³School of Informatics and Computing, Indiana University, Purdue University Indianapolis, United States

Submitted to Journal:

Frontiers in Genetics

Specialty Section:

Statistical Genetics and Methodology

Article type:

Original Research Article

Manuscript ID:

782953

Received on:

25 Sep 2021

Revised on:

09 Nov 2021

Journal website link:

www.frontiersin.org



Conflict of interest statement

The authors declare that the research was conducted in the absence of any commercial or financial relationships that could be construed as a potential conflict of interest

Author contribution statement

Shan Cong: Conceptualization, Methodology, Software, Formal analysis, Validation, Writing - Original Draft. Xiaohui Yao: Formal analysis, Validation, Writing - Review & Editing. Jingwen Yan: Data Curation, Resources Writing - Review & Editing. Linhui Xie: Data Curation, Software, Writing - Review & Editing. Li Shen: Supervision, Conceptualization, Methodology, Writing - Review & Editing.

Keywords

causal inference, Body Mass Index, Genome-Wide Association Study, human connectomics, network segregation

Abstract

Word count: 253

Background: Human brain structural connectivity is an important imaging quantitative trait for brain development and aging. Mapping the network connectivity to the phenotypic variation provides fundamental insights in understanding the relationship between detailed brain topological architecture, function, and dysfunction. However, the underlying neurobiological mechanism from gene to brain connectome, and to phenotypic outcomes, and whether this mechanism changes over time, remain unclear.

Methods: This study analyzes diffusion-weighted imaging data from two age-specific neuroimaging cohorts, extracts structural connectome topological network measures, performs genome-wide association studies of the measures, and examines the causality of genetic influences on phenotypic outcomes mediated via connectivity measures.

Results: Our empirical study has yielded several significant findings:

- 1) It identified genetic makeup underlying structural connectivity changes in the human brain connectome for both age groups. Specifically, it revealed a novel association between the minor allele (G) of rs7937515 and the decreased network segregation measures of the left middle temporal gyrus across young and elderly adults, indicating a consistent genetic effect on brain connectivity across the lifespan.
- 2) It revealed rs7937515 as a genetic marker for body mass index in young adults but not in elderly adults.
- 3) It discovered brain network segregation alterations as a potential neuroimaging biomarker for obesity.
- 4) It demonstrated the hemispheric asymmetry of structural network organization in genetic association analyses and outcomerelevant studies.

Discussion: These imaging genetic findings underlying brain connectome warrant further investigation for exploring their potential influences on brain-related complex diseases, given the significant involvement of altered connectivity in neurological, psychiatric and physical disorders.

Contribution to the field

The major contributions of this study are fivefold: (1) We elucidate the neurobiological pathway from SNPs to brain connectome, and to phenotypic outcomes. By integrating connectomics and genetics, this study provides new genetic mechanism insights into understanding detailed brain topological architecture and encoding (or mapping) inter-regional connectivity in the genome. (2) We validate the study outcomes by examining genetic consistency and discrepancy for complex-network attributes between young adult cohort and elderly adult cohort, which illustrates genetic basis for human connectome in different life stages. (3) We demonstrate that body mass index (BMI, which is a well-known factor related to multiple complex diseases) is influenced by a locus rs7937515128 with network segregation attributes measured at the left middle temporal gyrus as mediators, which reveals the intermediate effects of brain connectivity in the pathway of outcome-relevant genetics. (4) We discover network segregation as important neuroimaging biomarker for BMI and weight-related issues, and illustrate the importance of the left middle temporal gyrus for BMI. (5) We demonstrate the hemispheric asymmetry of structural network organization in genetic association analyses and outcome-relevant studies.

This work (including open access publication fees) was supported in part by NIH R01 EB022574, R01 LM013463 and R21 AG066135; by NSF 1837964, 1942394, and 1755836; and Dr. Shen's research fund at University of Pennsylvania.

Ethics statements

Studies involving animal subjects

Generated Statement: No animal studies are presented in this manuscript.

Studies involving human subjects

Generated Statement: The studies involving human participants were reviewed and approved by Institutional Review Boards (IRB) at University of Pennsylvania. The patients/participants provided their written informed consent to participate in this study.

Inclusion of identifiable human data

Generated Statement: No potentially identifiable human images or data is presented in this study.

Data availability statement

Generated Statement: Publicly available datasets were analyzed in this study. This data can be found here: the ADNI website (http://adni.loni.usc.edu/) and the HCP website (https://www.humanconnectome.org/)..



Genetic Influence underlying Brain Connectivity Phenotype: A Study on Two Age-Specific Cohorts

Shan Cong 1,† , Xiaohui Yao 1,† , Linhui Xie 2 , Jingwen Yan 3 , Li Shen 1,* , for the Alzheimer's Disease Neuroimaging Initiative *

- ¹Department of Biostatistics, Epidemiology and Informatics, Perelman School of Medicine, University of Pennsylvania, Philadelphia, PA 19104, USA.
- ²Department of Electrical and Computer Engineering, School of Engineering, Indiana University Purdue University Indianapolis, Indianapolis, IN 46202, USA.
- ³Department of BioHealth Informatics, School of Informatics and Computing, Indiana University Purdue University Indianapolis, Indianapolis, IN 46202, USA.
- * The Alzheimer's Disease Neuroimaging Initiative: Data used in preparation of this article were obtained from the Alzheimer's Disease Neuroimaging Initiative (ADNI) database (adni.loni.ucla.edu). As such, the investigators within the ADNI contributed to the design and implementation of ADNI and/or provided data, but did not participate in analysis or writing of this report. A complete listing of ADNI investigators can be found at: http://adni.loni.usc.edu
- † These authors have contributed equally to this work and share first authorship

Correspondence*: Li Shen, PhD B306 Richards Building 3700 Hamilton Walk Philadelphia, PA 19104 (+1) 215-573-2956 li.shen@pennmedicine.upenn.edu

2 ABSTRACT

- 3 Background: Human brain structural connectivity is an important imaging quantitative trait
- 4 for brain development and aging. Mapping the network connectivity to the phenotypic variation
- 5 provides fundamental insights in understanding the relationship between detailed brain topological
- 6 architecture, function, and dysfunction. However, the underlying neurobiological mechanism from
- 7 gene to brain connectome, and to phenotypic outcomes, and whether this mechanism changes
- 8 over time, remain unclear.
- 9 Methods: This study analyzes diffusion-weighted imaging data from two age-specific
- 10 neuroimaging cohorts, extracts structural connectome topological network measures, performs
- 11 genome-wide association studies of the measures, and examines the causality of genetic
- influences on phenotypic outcomes mediated via connectivity measures.
- 13 Results: Our empirical study has yielded several significant findings: 1) It identified genetic
- 14 makeup underlying structural connectivity changes in the human brain connectome for both age
- groups. Specifically, it revealed a novel association between the minor allele (G) of rs7937515
- and the decreased network segregation measures of the left middle temporal gyrus across

- young and elderly adults, indicating a consistent genetic effect on brain connectivity across the
- lifespan. 2) It revealed rs7937515 as a genetic marker for body mass index in young adults 18
- but not in elderly adults. 3) It discovered brain network segregation alterations as a potential 19
- neuroimaging biomarker for obesity. 4) It demonstrated the hemispheric asymmetry of structural 20
- network organization in genetic association analyses and outcome-relevant studies. 21
- **Discussion:** These imaging genetic findings underlying brain connectome warrant further 22
- investigation for exploring their potential influences on brain-related complex diseases, given the 23
- significant involvement of altered connectivity in neurological, psychiatric and physical disorders. 24
- 25 Keywords:Human Connectomics; Network Segregation; Genome-Wide Association Study; Body Mass Index; Causal inference

1 INTRODUCTION

- Brain structural connectivity is a major organizing principle of the nervous system. Estimating interregional
- neural connectivity, reconstructing geometric structure of fiber pathways, and mapping the network 27
- 28 connectivity to corresponding inter-individual variabilities provide fundamental insights in understanding
- detailed brain topological architecture, function and dysfunction. A large body of research has been 29
- devoted to extracting and investigating macro-scale brain networks from diffusion-weighted imaging (DWI) 30
- data (Xie et al., 2018; Jiang et al., 2019; van den Heuvel et al., 2019; Elsheikh et al., 2020; Bertolero 31
- et al., 2019), and various behavioral, neurological and neuropsychiatric disorders have been linked to the 32
- disrupted brain connectivity (Jiang et al., 2019; van den Heuvel et al., 2019). As structural changes of brain 33
- connectivity are phenotypically associated with massive complex traits across different categories, the 34
- brain-wide connectome has been extensively studied. 35
- It is worth noting that human brain connectome re-configures its network structure dynamically and 36
- adaptively in response to genetic, lifestyle, environmental factors (Cauda et al., 2018; Cohen and D'Esposito, 37
- 2016), brain development and aging (Sala-Llonch et al., 2015; Alloza et al., 2018; Varangis et al., 2019). 38
- However, the underlying neurobiological mechanism from gene to brain connectome, and to cognitive and 39
- behavioral outcomes, and whether this mechanism changes over time, remain unclear. To bridge this gap, 40
- we perform a genetic study of brain connectome phenotypes on two different age-specific cohorts: one 41
- contains healthy young adults (age: 28.7 ± 3.6), and the other contains elderly participants (age: 73.8 ± 7.0). 42
- Our goal is to identify genetic factors affecting brain connectivity and examine their consistency and 43
- discrepancy between these two age-specific groups. 44
- 45 Emerging advances in multimodal brain imaging, high throughput genotyping and sequencing techniques
- provide exciting new opportunities to ultimately improve our understanding of brain structure and neural 46
- 47 dynamics, their genetic architecture and their influences on cognition and behavior (Shen and Thompson,
- 2020). Present studies investigating direct associations among human connectomics, genomics and clinical 48
- phenotyping are primarily focused on four aspects: (1) estimating genetic heritability of basic connectome 49
- measures such as number of fibers, length of fibers and fractional anisotropy (FA) (Jahanshad et al., 50
- 2013; Thompson et al., 2013; Elliott et al., 2018); (2) discovering pairwise univariate associations between 51
- single nucleotide polymorphisms (SNPs) and imaging phenotypic traits such as above mentioned basic 52
- connectome measures at each edge (Jahanshad et al., 2013; Karwowski et al., 2019) and white matter 53
- properties at each voxel (Alloza et al., 2018; Kochunov et al., 2010; Guo et al., 2020); (3) discovering 54
- pairwise univariate associations between SNPs and clinical phenotypes such as cognitive or behavioral 55
- outcomes (Jahanshad et al., 2013; Elsheikh et al., 2020); and (4) discovering pairwise univariate associations 56

60 61

62 63

64 65

66

67

68 69

70

71

72

73

74

75

76 77

78

79 80

81

82

83

84

85

86

87 88

89

90

91

92 93

94

96

97

99

100

57 between basic connectome measures and clinical phenotypes (Jiang et al., 2019; van den Heuvel et al., 2019).

Among the studies mentioned above, there exist two major limitations. First, these studies were conducted based on basic connectome measures such as number of fibers, length of fibers and FA, but the complexnetwork attributes were overlooked, which included network segregation, integration, centrality and resilience and important network components such as hubs, communities, and rich clubs (Sporns, 2013). These attributes were extensively adopted to detect network integration and segregation, quantitatively measure the centrality of network regions and pathways, characterize patterns of local anatomical circuitry, and test resilience of networks to insult (Rubinov and Sporns, 2010). Second, these studies performed analyses by examining the association between an independent variable (e.g. SNP) and a dependent variable (e.g. cognitive or behavioral outcome), without taking into consideration the mediator(s) linking these variables (Baron and Kenny, 1986). Mediation analysis can help identify the underlying mechanism of outcome-relevant genetic effects implicitly mediated by neuroimaging phenotypes (e.g. connectome measures). Of note, mediation analysis requires the independent variable to be significantly associated with both the dependent variable and the mediator. This makes applying it in brain neuroimaging studies a challenge due to the modest effect size of an individual genetic variant on both behavioral and imaging phenotypes (Saykin et al., 2015; Cong et al., 2018), as well as limited size of the sample with all diagnostic, imaging and genetic data available.

With the demand of measuring complex-network attributes, a few recent genome-wide association studies (GWAS) (Elsheikh et al., 2020; Bertolero et al., 2019) recognized the first problem mentioned above and adopted quantitative measurement approaches for complex-network attributes, and treated the attributes as neuroimaging traits for the explorations of complex imaging genomic associations. They successfully identified a number of loci susceptible for Alzheimer's Disease (Elsheikh et al., 2020), and demonstrated the associations between loci and segregated network patterns, which may be involved in brain development, evolution, and disease (Bertolero et al., 2019). However, a notable limitation is that these studies only focus on the brain networks of either young or elderly participants, as a result, their study outcomes are lack of validations in multiple data sets. Since there is an age-related discrepancy for genetic effects on human connectome alterations across lifespan (Varangis et al., 2019), it remains an under-explored topic to examine genetic consistency and discrepancy for complex-network attributes among cohorts different in age. Another factor that may cause discrepancy in the network architecture is the hemispheric asymmetry (Jiang et al., 2019), and the hemispheric asymmetry of network organization has been linked to development processes (Zhong et al., 2017) and neuropsychiatric disorders (Sun et al., 2017). It remains a challenge to understand the genetic basis for the network attributes of two hemispheres as they may be distinctively correlated to cognition level, physical and psychological development.

Among a large number of complex-network attributes, it has been well documented in recent literatures (Xie et al., 2018; Cohen and D'Esposito, 2016) that segregation of neural information such as modularity, transitivity, clustering coefficients and local efficiency represent the connectivity of local network communities that are intrinsically densely connected and strongly coupled. A converging evidence (Cohen and D'Esposito, 2016; Karwowski et al., 2019) is shown that local, within-network communication is critical for motor execution, whereas integrative, between-network communication is critical for measuring connectome (Bertolero et al., 2019). Thus, network segregation is thought to be essential for describing and understanding of complex neural connectome systems (Sporns, 2013). In addition, segregation measures are highly reliable and heritable network attributes (Xie et al., 2018), and these measures have been linked to the disruption of neural network connectivity in brain

127

128

129

130

131

132

133

134 135

development, evolution, disease (Bertolero et al., 2019; Cohen and D'Esposito, 2016; Mak et al., 2016), and immunodeficiency (Bell et al., 2018). Given the importance of network segregation, in this study, we 102 first focus on quantifying measures of network segregation, analyzing heritability of segregation measures 103 and performing genetic association analyses by treating them as neuroimaging traits. Then, our next priority is to explore the genetic basis for the rest of the complex-network attributes (e.g. integration, centrality and 105 resilience). 106

To overcome the challenges mentioned above, this study aims to develop and implement computational 107 and statistical strategies for a systematic characterization of structural connectome optimized for imaging 108 genetic studies, and to determine genetic basis of structural connectome. Specifically, the framework 109 is organized and described in Figure 1, and the primary goals are to address the following six critical 110 issues: (a) construction of basic network connectivity with diffusion tractography, (b) systematic extraction 111 of complex-network attributes, (c) heritability analysis of complex-network attributes, (d) genome-wide 112 113 association studies of quantitative endophenotypes, (e) examination of mediation effect that intermediately bridges genes and outcomes, and (f) identification of outcome-relevant neuroimaging biomarkers. Given 114 the enormously broad scope of brain connectome, our focus is on studying (1) static tractography-based 115 structural connectome and complex-network attributes characterizing segregation, integration, centrality 116 and resilience; (2) genetic consistency and discrepancy for complex-network attributes among cohorts 117 different in age; and (3) mediation effects of network attributes on outcome-relevant genetics. 118

- The major contributions of this study are fivefold: 119
- 120 • New challenges in human connectome: we elucidate the neurobiological pathway from SNPs to brain connectome, and to phenotypic outcomes. By integrating connectomics and genetics, this study provides new genetic mechanism insights into understanding detailed brain topological architecture, 122 and encoding (or mapping) inter-regional connectivity in the genome. 123
- New genetic insights for brain phenotype: we validate the study outcomes by examining genetic 124 consistency and discrepancy for complex-network attributes between young adult cohort and elderly 125 adult cohort, which illustrates the genetic basis for human connectome in different life stages. 126
 - Biological findings: we treat network segregation measures as imaging quantitative traits (iQT), and demonstrate that body mass index (BMI, which is related to multiple complex diseases (Emmerzaal et al., 2015; Stenholm et al., 2017)) is influenced by a locus rs7937515 with network segregation attributes (e.g. clustering coefficient and local efficiency) measured at the left middle temporal gyrus as mediators, which reveals the intermediate effects of brain connectivity in the pathway of outcomerelevant genetics.
 - Biological findings: we discover network segregation as an important neuroimaging biomarker for BMI and weight-related disorders, and illustrate the importance of the left middle temporal gyrus for
- Biological findings: we demonstrate the hemispheric asymmetry of structural network organization in 136 genetic association analyses and outcome-relevant studies. 137

2 MATERIALS AND METHODS

2.1 Study datasets 138

139 With the purpose of examining genetic consistency and discrepancy for complex-network attributes between young and elderly adults, and illustrating genetic basis for human connectome in different life 140

- 141 stages, our analysis was respectively conducted on Human Connectome Project (HCP) database for young
- 142 adults and Alzheimer's Disease Neuroimaging Initiative (ADNI) database for elderly adults.

143 2.1.1 HCP young adult dataset

- HCP (Van Essen et al., 2013) is a major endeavor to map macroscopic human brain circuits and
- their relationship to behavior in a large population. It aims to reveal the neural pathways that underlie
- 146 brain function and behavior, by acquiring and analyzing human brain connectivity from high-quality
- 147 neuroimaging data in healthy young adults. The HCP datasets serve as a key resource for the neuroscience
- 148 research community, as it provides valuable resources for characterizing human brain connectivity and
- 149 function, their relationship to behavior, and their heritability and genetic underpinnings, which enables
- 150 discoveries of how the brain is wired and how it functions in different individuals.

151 2.1.2 ADNI elderly adults data set

- Alzheimer's Disease Neuroimaging Initiative (ADNI) database was initially launched in 2004 as a
- public-private partnership, and led by the Principal Investigator Michael W. Weiner, MD. One primary aim
- of ADNI has been to examine whether serial imaging biomarkers extracted from MRI, positron emission
- 155 tomography (PET), other biological markers, and clinical and neuropsychological assessment can be
- 156 combined to measure the progression of mild cognitive impairment (MCI) and early AD. For up-to-date
- 157 information, see www.adni-info.org.

158 2.2 Demographics

- We initially downloaded 981 subjects from HCP database, including a part of twin subjects, then one
- 160 individual from each family was randomly selected and excluded. As a result, 275 unrelated participants
- 161 were selected for further population-based genetic analyses. ADNI data were collected by selecting the
- 162 participants who had both genotype data and baseline DWI data at their first visit, family relationship
- 163 was also removed in the same way as described above for HCP data filtration. Detailed characteristic
- 164 information and the number of subjects in each data cohort are shown in Table 1. In this study, we
- analyzed a total of 275 participants (age: 28.7 ± 3.6 ; gender: 137 male, 138 female; education: 15.1 ± 1.6)
- 166 from the HCP database, and a total of 178 participants (age: 73.8 ± 7.0 ; gender: 108 male, 70 female;
- education: 16.0 ± 2.8) from the ADNI database. This study was approved by institutional review boards of
- 168 all participating institutions, and written informed consent was obtained from all participants or authorized
- 169 representatives.

170

2.3 Genotyping data acquisition and processing

171 2.3.1 HCP young adults dataset

- HCP samples were genotyped using MEGA array with PsychChip and ImmunoChip content. 1,141
- 173 genotype data was downloaded from dbGAP. Quality control was performed in PLINK v1.90 (Purcell et al.,
- 174 2007) using the following criteria: 1) call rate per marker $\geq 98\%$, 2) minor allele frequency (MAF) $\geq 5\%$,
- 175 3) Hardy Weinberg Equilibrium (HWE) test $P \le 1.0E$ -6, and 4) call rate per participant $\ge 98\%$. Variants
- with no "rs" number, and samples with evidence of identity-by-descent (IBD) ≥ 0.25 or heterozygosity
- 177 rate ± 3 standard deviations from the mean were further excluded. Following quality control process, the
- the position of the mean were rather enough quality control process, the
- 178 number of samples with genotype data reduced to 327, we then checked the missing data by matching
- 179 subjects information between phenotype and genotype data. As a result, this study comprised a total of 327
- 180 unrelated subjects and 515,956 SNPs.

181 2.3.2 ADNI elderly adults dataset

- 182 Genotyping data were obtained from the ADNI database (adni.loni.usc.edu). They were quality-
- 183 controlled as described in (Yao et al., 2020; Cong et al., 2020). We then performed imputation to maximize
- the number of overlaps between HCP GWAS findings and ADNI SNPs, see (Yao et al., 2019) for details.
- 185 Briefly, genotyping was performed on all ADNI participants following the manufacturer's protocol using
- 186 blood genomic DNA samples and Illumina GWAS arrays (610-Quad, OmniExpress, or HumanOmni2.5-
- 187 4v1) (Saykin et al., 2010). Quality control was performed in PLINK v1.90 (Purcell et al., 2007) using
- 188 the following criteria: 1) call rate per marker $\geq 95\%$, 2) minor allele frequency (MAF) $\geq 5\%$, 3) Hardy
- Weinberg Equilibrium (HWE) test P \leq 1.0E-6, and 4) call rate per participant \geq 95%. In total, 5,574,300
- 190 SNPs were included for further targeted genetic association analysis.

2.4 Tractography and network construction

192 2.4.1 Tractography

191

- 193 We downloaded high spatial resolution DWI data and genotype data from both HCP and ADNI databases.
- 194 DWI data from HCP was processed following the MRtrix3 guidelines (Tournier et al., 2012), detailed
- procedures have been previously reported (Xie et al., 2018) and are briefly described below: (1) generating
- 196 a tissue-segmented image; (2) estimating the multi-shell multi-tissue response function and performing
- 197 the multi-shell multi-tissue constrained spherical deconvolution; (3) generating the initial tractogram
- and applying the successor of Spherical-deconvolution Informed Filtering of Tractograms (SIFT2)
- 199 methodology (Smith et al., 2015); and (4) mapping the SIFT2 output streamlines onto the MarsBaR
- automated anatomical labeling (AAL) atlas (Tzourio-Mazoyer et al., 2002) with 90 ROIs to produce the
- 201 structural connectome with edge value equal to the mean fractional anisotropy (FA).
- DWI data from ADNI was acquired following the scanning protocols described in (Elsheikh et al., 2020),
- and processed following the procedures discussed in (Yan et al., 2018). Tractography was performed in
- 204 Camino (Cook et al., 2006) based on white matter fiber orientation distribution function (ODF). As Camino
- 205 adopted a deterministic approach, streamlines were modeled with a multi-tensor modeling approach (voxels
- 206 fitted up to three fiber orientations, this way accounting for most of the fiber-crossings) of the ODF data.
- 207 To generate a comparable tractography, the streamlines were also mapped onto AAL atlas with 90 ROIs to
- 208 produce the structural connectome with edge value equal to the mean FA.

209 2.4.2 Network construction

- Network was created and defined by connectivity matrix M where M_{ij} stores the connectivity measure
- 211 between ROIs i and j. As described in the previous section, we considered FA for defining M_{ij} . Since
- 212 the diffusion tensor is a symmetric 3×3 matrix, it can be described by its eigenvalues (λ_1 , λ_2 and λ_3)
- 213 and eigenvectors $(v_1, v_2 \text{ and } v_3)$ for tractography analysis. FA at edge-level is an index for the amount of
- 214 diffusion asymmetry within a voxel, defined in terms of its eigenvalues:

$$FA = \sqrt{\frac{(\lambda_1 - \lambda_2)^2 + (\lambda_2 - \lambda_3)^2 + (\lambda_1 - \lambda_3)^2}{2(\lambda_1^2 + \lambda_2^2 + \lambda_3^2)}}.$$
 (1)

- 215 Thus, mean FA is a normalized measure of the fraction of the tensor's magnitude due to anisotropic
- 216 diffusion, corresponding to the degree of anisotropic diffusion or directionality.

2.5 Complex-network attributes

- With an undirected and weighted connectivity matrix M (defined in Section 2.4.2), we assessed a 218
- 219 comprehensive set of network features such as segregation (e.g. transitivity, clustering coefficients,
- local efficiency and modularity), integration (e.g. global efficiency), centrality (e.g. eigen centrality) 220
- and resilience (e.g. assortativity) of the structural connectome using Brain Connectivity Toolbox 221
- (BCT) (Rubinov and Sporns, 2010). Given the importance and priority of segregation measures in this study, 222
- we only introduced the definitions of segregation measures, and the definitions of the rest complex-network 223
- attributes were explained in (Rubinov and Sporns, 2010). 224
- For the following sub-sections, we define N as the set of all nodes in the network, n as the number of 225
- 226
- nodes, t_i as geometric mean of triangles around node i ($t_i = \frac{1}{2} \sum_{j,h \in N} \left(M_{ij} M_{ih} M_{jh} \right)^{1/3}$), k_i as weighted degree of i ($k_i = \sum_{j \in N} M_{ij}$), a_{ij} as the connection status between i and j ($a_{ij} = 1$ when link (i,j) exists, 227
- $a_{ij}=0$ otherwise), d_{ij} as shortest weighted path length between i and j ($d_{ij}=\sum_{a_{uv}\in g_{i\to j}}f\left(M_{uv}\right)$, where f is a map from weight to length and $g_{i\to j}$ is the shortest weighted path between i and j). 228
- 229

2.5.1 Transitivity 230

- Transitivity measures the ratio of triangles to triplets in the network. By following the definition 231
- in (Newman, 2003): 232

$$T = \frac{\sum_{i \in N} 2t_i}{\sum_{i \in N} k_i (k_i - 1)},$$
(2)

- where T is the transitivity measured at network level.
- Clustering coefficient 2.5.2 234
- 235 Clustering coefficient measures the degree to which nodes in a network tend to cluster together by
- evaluating the fraction of triangles around a node and is equivalent to the fraction of node's neighbors that 236
- are neighbors of each other. By following the definition in (Onnela et al., 2005): 237

$$C = \frac{1}{n} \sum_{i \in N} C_i = \frac{1}{n} \sum_{i \in N} \frac{2t_i}{k_i (k_i - 1)},$$
(3)

- where C_i is the clustering coefficient of node i and C is the clustering coefficient measured at network
- level. 239
- 2.5.3 Local efficiency 240
- Local efficiency measures the efficiency of information transfer limited to neighboring nodes by evaluating 241
- the global efficiency computed on node neighborhoods. By following the definition in (Latora and Marchiori, 242
- 2001): 243

$$E_{\text{loc}} = \frac{1}{n} \sum_{i \in N} \frac{\sum_{j,h \in N, j \neq i} (M_{ij} M_{ih} \left[d_{jh} (N_i) \right]^{-1})^{1/3}}{k_i (k_i - 1)}, \tag{4}$$

- where E_{loc} is the local efficiency of node i, and $d_{jh}(N_i)$ is the length of the shortest path between j and h,
- that contains only neighbors of i.

246 2.5.4 Modularity

Modularity measures network segregation into distinct networks, and it is a statistic that quantifies the degree to which the network may be subdivided into such clearly delineated groups (Newman, 2006):

$$Q = \frac{1}{l} \sum_{i,j \in N} \left[M_{ij} - \frac{k_i k_j}{l} \right] \delta_{m_i, m_j}, \tag{5}$$

249 where Q is the modularity measured at network level, m_i is the module containing node i, and $\delta_{m_i,m_j}=1$ 250 if $m_i=m_j$, and 0 otherwise.

251 2.6 Heritability Analysis

252

253254

255

256

257258

259

260

261

262263

264

265

266

267

268

276

277

278

279

280

281

282

283

Heritability analysis focused on identifying highly heritable measures of structural brain networks, and it was a commonly adopted and critical measurement to describe properties of the inheritance of iQT. An iQT such as network attributes must be heritable, which was defined as the proportion of phenotypic variance due to genetic differences between individuals (Jørstad and Næevdal, 1996). In this study, we estimated heritability of four segregation measures from twin subjects in the HCP young adult cohort (N=350, 232 mono-zygotic twins, 118 di-zygotic twins) and SOLAR-Eclipse software (Kochunov et al., 2015) was employed for this task. The inputs to this software included phenotype traits, covariates measures and a kinship matrix indicating the pairwise relationship between twin individuals. A maximum likelihood variance decomposition method was applied to estimate the variance explained by additive genetic factors and environmental factors respectively. The output from SOLAR-Eclipse included heritability (h2), standard error and the corresponding significance p-value for each feature. We estimated the heritability of connectomic features, including transitivity, clustering coefficients, local efficiency and modularity. Since many previous studies had reported the effect of age (linear nonlinear), gender and their interactions on structural brain connectivity (Zhao et al., 2015; Lopez-Larson et al., 2011; Gong et al., 2011; Burzynska et al., 2010), all heritability analyses were performed with age, age², sex, age×sex and age²×sex as covariates. In addition, we extracted the total variance explained by all covariate variables.

2.7 Brain connectome genetic association analysis

HCP cohort: GWAS on the brain network segregation measures of the 90 ROIs were performed using linear regression under an additive genetic model in PLINK v1.90 (Purcell et al., 2007). Age, gender and education were included as covariates. Our GWAS was focused on analyzing the following network segregation measures: (1) modularity and transitivity, which were network-level measures; and (2) clustering coefficient and local efficiency, which were node-level measures. As a result, in total, we have $2 + 90 \times 2 = 182$ measures. Our post-hoc analysis used Bonferroni correction for correcting the genome-wide significance (GWS) for the number of quantitative traits (i.e., 5E-8/182=2.75E-10).

ADNI cohort: Genetic findings of the segregation measures from HCP young adult dataset were treated as genotypic candidates and segregation measures at specific ROIs as phenotypic candidates, we further examined in ADNI elderly adult dataset regarding their associations. Apart from including age, gender and education as covariates, we also added diagnostic status into the linear regression model, as a large part of ADNI participants suffered from cognitive disorders. By validating the genetic findings from HCP data using ADNI participants, we examined genetic consistency and discrepancy for network segregation attributes between young and elderly adults, which illustrated the consistency and discrepancy of genetic basis for human connectome in different life stages.

291

292 293

297

298

309

310

284 In addition, the validated genetic findings were used to further explore connectivity variances with all 285 important complex-network attributes excepting segregation measures such as integration (e.g. global efficiency and network density), centrality (e.g. eigen centrality) and resilience (e.g. assortativity), and we 286 287 examined the targeted genetic basis on certain brain ROIs (e.g. middle temporal gyrus). As previously 288 stated, linear regression models were used. In particular, we applied additive genetic models implemented in PLINK v1.90, with age, gender, education as covariates. 289

2.8 **Mediation analysis**

To examine the causal assumption, we followed the Baron-Kenny procedure (Baron and Kenny, 1986) to perform standard mediation analysis to identify the mediated effect, and we treated iQTs (e.g. network segregation measures) as mediating variables, which intermediately linked the pathological path from 294 genetic findings to clinical phenotypes. Specifically, we constructed a set of candidate SNPs which were found significantly associated to segregation measures in both young and elderly participants, and we 295 296 constructed a set of candidate clinical phenotyping information by extracting overlapped clinical outcomes collected in both HCP and ADNI databases. We then employed the mediation model to detect the indirect effect of loci on clinical outcomes via iQT.

Specifically, mediation analysis was performed using the non-parametric bootstrap approximation with 299 the R 'mediation' package developed by Imai et al. (2010). Let y be the dependent variable which was a 300 clinical outcome in our study, x be the independent variable which was a candidate SNP, z be the covariates 301 (age, gender and education), and M be the mediating variable which was brain iQT. The mediation analysis 302 was conducted in 3 steps: 303

- 304 1) fit a linear model to regress the mediating variable M against SNP x while controlling for z;
- 2) fit a linear model to regress the clinical outcome y against SNP x while controlling for z; 305
- 3) adopted the non-parametric bootstrap approximation to estimate the direct effect, mediation effect, 306 proportion of total effect via mediation, their 95% confidence intervals (CI) and p values, by conducting 307 1,000 simulations. 308

2.9 Outcome-relavent brain connectome association analysis

behavioral outcomes, we performed pairwise univariate association analysis between network segregation 311 attributes and outcome data. We selected BMI and Mini-Mental State Examination (MMSE) as outcomes 312 as they were not only measures available in both HCP and ADNI cohorts but also important quantitative 313 traits related to complex diseases such as weight-related disorders as well as neurological and psychiatric 314 disorders. We used linear regression to regress the phenotypic outcomes against network segregation 315 measures for both HCP and ADNI datasets, and explored outcome-relevant brain neuroimaging biomarkers. 316 By comparing young and elderly participants, we illustrated the consistency and discrepancy of human 317

To discover the outcome-relevant biomarkers which mapped brain connectivity alterations to cognitive or

brain connectome in different ages regarding on BMI and MMSE variations.

3 **RESULTS**

3.1 Heritability of network segregation 319

320 As illustrated in Figure 1, we examined segregation measures estimated at both network-level and node-321 level prior to GWAS. All of the segregation measures such as clustering coefficients (node-level), local

- 322 efficiencies (node-level), transitivity (network-level) and modularity (network-level) showed significantly
- 323 high heritability after Bonferroni correction (p<0.05/182 = 2.75E-04). The mean (\pm std) heritability of
- 324 182 segregation measures (h2 score) was $0.81(\pm 0.05)$, and more detailed results of heritability analysis
- 325 were listed in Supplementary Table. We included all 182 segregation measures in the subsequent GWAS
- 326 analysis.

3.2 GWAS of network segregation in HCP young adults

- In the HCP cohort, genome-wide associations between 515,956 SNPs and 182 structural network
- 329 segregation measures were assessed under the additive genetic model and controlled for age, gender and
- 330 education. GWAS identified 20 significant associations between 10 SNPs and 7 segregation measures
- 331 (Table 2), after correcting the genome-wide significance (GWS) for the number of phenotypes using
- Bonferroni method (i.e., p< 5E-08/182 = 2.75E-10). Respectively shown in Figure 2 were Manhattan plots
- 333 of GWAS results of clustering coefficient and local efficiency measured in left middle temporal gyrus.
- 334 GWAS of HCP data showed high consistency for clustering coefficient and local efficiency, where nine
- 335 SNP-ROI associations were discovered for these two segregation measures. After Bonferroni correction,
- 336 there was no significant finding for the network level segregation measures (i.e., transitivity and modularity).

337 3.3 Targeted genetic association of segregation in ADNI elderly adults

- 338 Given the list of significant findings from the aforementioned GWAS of HCP segregation measures, we
- 339 further examined their statistical significance in the ADNI cohort to identify brain network relevant genetic
- 340 variants which were consistent for brain aging. We assessed the associations of 15 out of 20 HCP GWAS
- 341 findings in ADNI cohort, as three SNPs (rs4841664, rs1461192 and rs147446959 are corresponding to
- 342 5 associations in Table 2) were not included in ADNI genotyping data. Associations of rs7937515 with
- 343 clustering coefficient and local efficiency measured in left middle temporal gyrus were duplicated and
- validated in ADNI cohort with p values of 1.63E-03 and 1.34E-03, respectively, where the Bonferroni
- 345 corrected significant level p < 0.05/15 = 3.33E-03 was applied (Table 2).
- The minor allele G of rs7937515 (rs7937515-G) was associated with lower level of both clustering
- 347 coefficient and local efficiency, compared to its major allele A (Figure 3). We will discuss the risk effect of
- 348 rs7937515-G on brain function and dysfunction in the discussion section.

349 3.4 Mediation analysis

- 350 According to the genetic association results from the HCP and ADNI subjects, we identified a common
- 351 genetic finding SNP rs7937515, which was associated with two segregation measures in left middle
- 352 temporal gyrus (e.g. clustering coefficient and local efficiency). In addition, we extracted two common
- 353 behavioral and cognitive outcome measures (e.g. BMI and MMSE) by comparing the outcome evaluation
- 354 methods across the HCP and ADNI databases. Thus, in this section, we had two major focuses: (1)
- exploring the genetic effect of SNP rs7937515 on outcomes including BMI and MMSE, and gaining deeper
- 356 insights to the molecular mechanisms of the identified genetic variant, and (2) examining the mediated
- 357 effect of iQTs (e.g. segregation measures) and illustrating their implicit effects in (1).
- To achieve those two goals, mediation analysis of outcome was performed for evaluating both the direct
- and implicit effects of rs7937515 on outcomes (i.e., BMI and MMSE) through segregation measurements
- 360 in left middle temporal gyrus. Mediation analysis required the independent variable (i.e., rs7937515) to
- 361 be significantly associated with both the dependent variable (i.e., BMI or MMSE) and the mediator (i.e.,

390

391

segregation measurements). Below we respectively reported the mediation results analyzed from both HCP and ADNI data.

For the first focus, the minor allele G of rs7937515 was significantly associated with the increased BMI 364 in HCP cohort (p = 1.62E-03; Figure 4A). The same increasing trend was also observed from the ADNI 365 data, although the association between rs7937515 and BMI was not significant (p = 0.22; Figure 4B). For 366 the second focus, Figure 5 illustrated the results of mediation analysis with BMI as an outcome measure, 367 368 from which both clustering coefficient and local efficiency of the left middle temporal gyrus demonstrated the significant intermediate roles between rs7937515 and BMI, with mediation effects of 0.98 (95%CI 369 = [0.06, 2.29], p = 3.60E-02) and 0.99 (95%CI = [0.02, 2.11], p = 4.60E-02), respectively. There was no 370 371 significant association between rs7937515 with MMSE in the HCP young adult dataset, so no mediation 372 analysis regarding MMSE was performed. In the ADNI elderly adult dataset, there were no significant associations observed between rs7937515 with BMI nor MMSE; therefore it was not necessary to further 373 374 examine mediation effects.

Since the brain can be viewed as a predictor, a mediator, or outcome of a health condition (e.g., obesity)
(Lowe et al., 2019), it is unclear whether the brain regulates the condition (e.g., structural connectome
alteration considered as a mediator for a physical condition such as BMI), or, conversely, brain is affected
by the condition. For completeness, we also explored the potential reciprocal relationship from the other
direction. The above experiment was repeated with BMI as a mediator and connectivity measures as
outcomes. No significant findings were identified, and thus no evidence was observed for BMI as a
significant mediator between gene and brain connectivity.

3.5 Outcome-relevant neuroimaging biomaker discoveries

On one hand, for the HCP cohort, we respectively identified significantly negative associations (p< 0.05/4 = 1.25E-02) between BMI with clustering coefficient (p= 3.92E-05) and local efficiency (p= 4.57E-05) measured in left middle temporal gyrus. On the other hand, for the ADNI cohort, we examined the associations between BMI and the above mentioned segregation measures in a pair-wise manner, but there was no significant findings satisfying the corrected p threshold. Regarding the relationship between cognitive score (e.g. MMSE) and network segregation measures, there was no significant associations identified for both HCP and ADNI cohorts.

3.6 Targeted genetic association of other important network attributes in the left middle temporal gyrus

To review the genetic effect of SNP rs7937515 from different aspects of network connectivity attributes of 392 393 the left middle temporal gyrus, we assessed the relationship between rs7937515 and additional node-level measures on reported brain ROI (i.e., left middle temporal gyrus) as well as network-level measures in both 394 HCP and ADNI datasets. Table 3 showed association statistics of rs7937515 with segregation, integration, 395 centrality and resilience measures. After correcting for the number of examined network measures (i.e., 396 P < 0.05/9 = 5.56e-03), both HCP and ADNI identified significant associations between the targeted SNP 397 with global efficiency (integration) and transitivity (resilience), together with our previous finding that 398 rs7937515 was associated with segregation measures such as clustering coefficient and local efficiency, 399 our results showed the consistent genetic effect of rs7937515 on brain structural network segregation, 400 401 integration and resilience across aging. Besides the common findings between young and elderly adults, rs7937515 was associated with several other node-level and network-level attributes including network 402

406 407

408

409

410

411 412

413

414

415

416

density (integration) and eigenvector centrality (centrality) in HCP data, but not in ADNI. Our results suggested the possible genetic discrepancy for certain brain connectivities in different life stages.

3.7 Hemispheric asymmetry of brain connectome

In this study, we noticed a hemispheric asymmetry of outcome-relevant brain connectivity alterations in the left and right middle temporal gyrus (Table 3). Due to two brain regions (e.g. left and right MTG), two segregation measures (e.g. clustering coefficient and local efficiency) and one outcome measure (e.g. BMI), we applied a Bonferroni corrected p threshold in this section (p<5E-02/8=6.25E-03). In the HCP young adult cohort, for the left MTG, we respectively identified significant associations of BMI with clustering coefficient (p=3.92E-05), and with local efficiency (p=4.57E-05); for the right MTG, even though there were no significant associations of BMI with clustering coefficient (p=2.24E-02), and with local efficiency (p=2.90E-02), both clustering coefficient and local efficiency in left and right MTG showed negative associations with BMI. In the ADNI cohort, as reported in the previous section, network segregation was not associated with BMI, so it was not necessary and proper to conduct analyses regarding ADNI data in this section.

4 DISCUSSION

As summarized in Figure 1, prior to GWAS, we first performed heritability analysis for network attributes 417 screening, and only heritable measures of network segregation were treated as iQT for GWAS. Based on 418 419 experimental outcomes, all of the segregation measures were highly heritable: transitivity and modularity 420 were heritable at network level, clustering coefficient and local efficiency were heritable at all nodes, which suggested segregation measures were suitable for genetic analyses. Then, we performed GWAS of 421 segregation attributes in 275 HCP subjects, and identified several pairwise associations between SNPs and 422 423 iQTs as listed in Table 2. These GWAS findings were validated in 178 ADNI subjects. As a validation result, we identified several genetic consistency and discrepancy patterns for human connectome in different 424 life stages (as shown in Table 2). As common findings in both HCP young adult and ADNI elderly adult 425 cohorts, rs7937515 was negatively associated with clustering coefficient and local efficiency respectively 426 427 measured at left middle temporal gyrus. To the best of our knowledge, this was among the first GWAS of human brain high-level network measures across both young and elderly participants. As shown in 428 429 Figure 3(a,c), the minor allele G of rs7937515 was associated with decreased clustering coefficient and local efficiency of the left middle temporal gyrus in both young and elderly participants. As concluded 430 in (Varangis et al., 2019; Karwowski et al., 2019; Keown et al., 2017; Rudie et al., 2013), the weakness of 431 segregated network connectivity (e.g. modularity, clustering coefficient, and local efficiency) was linked 432 to multiple brain disorders such as age-related cognitive declines and autism spectrum disorder. Thus, 433 our GWAS findings for HCP young adults demonstrated that rs7937515 played a risk effect on human 434 network segregation. This neurorisk effect was also confirmed in a targeted genetic association analysis 435 for ADNI elderly participants (as shown in Figure 3 (b,d)), these common discoveries between HCP and 436 ADNI datasets suggested a consistent genetic risk effect across young and old life stages. 437

This study was further conducted by performing several post-hoc analyses in the following three aspects (shown as bottom sections in Figure 1): 1) examining genetic mechanisms for common outcome measures in the HCP and ADNI studies, and elucidating the mediated effect of iQTs for such outcome-relevant genetic association, 2) discovering outcome-relevant imaging biomarkers, and 3) exploring the genetic mechanisms of other important complex-network attributes.

444

445 446

447

448 449

450

451

452

453

454

455 456

457

458 459

460

461 462

463

464

465

466

467

468

469

470

471

472

473

474

475

476

477

478

479

480

481

482

For the first aspect, our goal was to elucidate the neurobiological pathway from SNPs to brain connectome, and to phenotypic outcome. In addition, we aimed to discover the role of iQTs in the outcome-relevant genetic associations by performing mediation analyses in both HCP and ADNI datasets. For the HCP young participants, we identified that BMI was positively associated with rs7937515 in the first step of mediation analysis, demonstrating a risk effect. rs7937515 located in the regions of FAM86C1/FOLR3 was previously discussed in literatures (Gao et al., 2015; Gao, 2017) and positively linked to waist circumference in the meta-analysis based on the Insulin Resistance Atherosclerosis Family Study (IRASFS) (Palmer et al., 2015), which was designed to investigate the genetic and environmental basis of insulin resistance and adiposity. FAM86C1 (Family With Sequence Similarity 86 Member C1) and FOLR3 (Folate Receptor Gamma) had been reported for their associations with various weight-related phenotypes such as bone mineral density (Li et al., 2019) and BMI (Mrozikiewicz et al., 2019; Hair, 2014), which closely related to osteoporosis (Li et al., 2019; Mrozikiewicz et al., 2019) and obesity (Gómez-Ambrosi et al., 2004). In the second and third steps of mediation analysis, we illustrated that BMI was indirectly influenced by rs7937515 (Figures 4 and 5), and iQTs such as clustering coefficient and local efficiency measured at the left middle temporal gyrus respectively played a mediating role. We also examined the genetic association with MMSE, but no evidence indicated any genetic associations to MMSE. In contrary, for the ADNI elderly participants, neither significant associations between rs7937515 and BMI nor MMSE were identified in the first step of mediation analysis, so there was not a necessary to examine mediated effect in this dataset. Our results demonstrated a disappearance of outcome-relevant genetic effect in the elderly participants, this discrepancy from young to elderly participants might due to the dominated influences from life style, environment or other non-genetic factors.

For the second aspect, recent studies (Lowe et al., 2019; Azevedo et al., 2019) showed that structural changes in brain tissues could affect food consumption behaviors and mediate BMI, which implied connectome alteration could be a causal agent and a promising imaging biomarker in this study. Thus, our goal was set to reveal the mapping between connectivity alterations and phenotypic outcome, and discover outcome-relevant imaging biomarkers. For young adult participants, segregation measures (e.g. clustering coefficient or local efficiency measured at left middle temporal gyrus) previously demonstrated their potential to play a mediating role in genetic association discoveries, in this step, we focused on examining their direct associations to the outcomes. Thus, we performed a targeted association analysis between the mentioned segregation measures and the common outcomes (e.g. BMI or MMSE) evaluated in both HCP and ADNI studies (Table 2) by employing linear regression models. For the young participants, clustering coefficient and local efficiency measured at left middle temporal gyrus were negatively associated with BMI. Similar observation was obtained in (Chen et al., 2018) which linked lower structural network segregation to obesity (higher BMI). Our findings suggested that there was a mapping between brain network segregation attributes and human physical conditions, and segregation features of the left middle temporal gyrus showed their potential as neuroimaging biomarkers to detect BMI-associated complex diseases such as dementias (Emmerzaal et al., 2015), cardiovascular disease, cancer, respiratory disease and diabetes (Stenholm et al., 2017). For elderly adult participants, no significant associations were identified between segregation measures and any outcomes, which suggested an interesting topic for further explorations.

Multiple regression analyses demonstrated that middle temporal gyrus was linked to weight-related issues. For example, Veit et al. (Veit et al., 2014) and Gómez-Apo et al. (Gómez-Apo et al., 2018) revealed that BMI, visceral fat and age were negatively associated with cortical thickness of the left middle temporal gyrus, Ou et al. (Ou et al., 2015) indicated that greater adiposity was associated with lower gray matter (GM) volumes in the middle temporal gyrus, Yokum et al. (Yokum et al., 2012) found positive correlation

499

500

501

502 503

504

505

506

507 508

509

510

511

512

513

514

515 516

517

518

519

520

521

522

523

524

525

526

527 528

529

between BMI and white matter (WM) volume in the middle temporal gyrus, Rapuano et al., 488 489 2016) illustrated left middle temporal gyrus was detected significantly greater activation in response to food commercials than to non-food commercials, Salzwedel et al. (Salzwedel et al., 2019) concluded that 490 491 maternal adiposity influenced neonatal brain functional connectivity in middle temporal gyrus, and Peven et al. (Peven et al., 2019) identified that cardiorespiratory fitness was negatively associated with functional 492 connectivity in the right middle temporal gyrus. To the best of our knowledge, our investigations for the 493 494 association between structural connectivity in the middle temporal gyrus and BMI was among the first weight-related studies with high-level imaging features measured from structural network connectivity, and 495 our results confirmed several previous findings analyzed from thickness data, T1-weighted MRI data, and 496 fMRI data. 497

For the third aspect, since there was an emerging interest in understanding the segregation and the integration of brain networks (Cohen and D'Esposito, 2016; Mohr et al., 2016) as well as other important network attributes such as centrality (Zuo et al., 2012) and resilience (Karwowski et al., 2019), our goal was to expand our focus on comprehensively discussed segregation attributes to a more complete set of network attributes including segregation, integration, centrality and resilience. For both node level network attributes measured at left and right middle temporal gyrus and global network attributes, we applied targeted genetic association analyses on global efficiency and density (integration, network level), betweeness and eigenvector centrality (centrality, node level) and assortativity coefficient (resilience, network level) of the structural connectivity. We identified several pairwise associations between rs7937515 and these network attributes in both HCP and ADNI datasets (Table 3), and noticed a significant association between rs7937515 and global efficiency in both datasets, which suggested that rs7937515 was involved into the dynamic fluctuations of segregation and integration of neural information. This finding partially answered an elusive question of revealing genetic basis for brain mechanisms of balancing network segregation and integration. Another worth noting finding was that rs7937515 was associationed density and eigenvector centrality respectively in our targeted analyses, while such associations were vanished in elderly participants, which suggested inconsistent genetic influences across different life stages.

With the awareness of the hemispheric asymmetry of network organization, a genetic basis to explain the differences in connectome between two hemispheres were under discovered. In this work, we identified an obvious inconsistency of genetic influences on human connectome in different brain hemispheres (Table 3). As reported in several recent studies (Jiang et al., 2019; Shu et al., 2015; Tian et al., 2011), the topological organizations of structural networks were not uniformly affected across brain hemispheres, which lead to a non-uniformly distributed destruction on neural network of the left and right hemispheres. Our finding gave an explanation from the point-view of genetics, with the potential for further investigations as many of the destruction on neural network (as iQT) were linked to cognitive and behavioral functions and dysfunctions, and their genetic mechanisms were still under discovered.

5 CONCLUSIONS

In this work, we constructed the structural network connectivity, extracted complex-network attributes and examined the heritability of network segregation measures. Then, we revealed a novel association between the minor allele (G) of rs7937515 and decreased network segregation measures of the left middle temporal gyrus across HCP young participants and ADNI elderly participants, which demonstrated a consistent genetic risk effect on brain network connectivity across lifespan. We elucidated the neurobiological pathway from SNP rs7937515 and genes *FAM86C1/FOLR3* to brain network segregation, and to BMI. In such pathway, we concluded a genetic risk effect on BMI due to their positive association, examined the

- mediated effect of network segregation measures, and discovered network segregation of the left middle 530
- 531 temporal gyrus as BMI-related neuroimaging biomarkers by identifying a negative association between
- them. We also examined genetic associations of a more complete set of important network attributes 532
- 533 including integration, centrality and resilience, and demonstrated the consistency and discrepancy in
- 534 genetic associations in brain aging. At last, we illustrated hemispheric asymmetry of network organization
- in both datasets in the aspect of genetic effect. 535
- 536 In sum, with the awareness that BMI is directly and indirectly associated to multiple complex diseases,
- this study performed a systematic analysis that integrated genetics, connectomics and phenotypic outcome 537
- data, with the goal of revealing biological mechanisms from the genetic determinant to intermediate brain 538
- connectomic traits and to the BMI phenotype at two different life stages. We identified the genetic effect 539
- of rs7937515 on human brain network segregation in both young and elderly participants and on BMI in 540
- young adult cohort. Our findings confirmed several previous genetic and imaging biomarker discoveries. 541
- 542 Moreover, we provided outcome-relevant genetic insights in the aspect of complex-network attributes of
- human brain connectome. Similar analytical strategies can be applied to future integrative studies linking 543
- genomics with connectomics, including the analyses of structural and functional connectivity measures, 544
- additional network attributes, longitudinal or dynamic connectomic features, as well as other types of brain 545
- imaging genomic data. 546

CONFLICT OF INTEREST STATEMENT

The authors have no actual or potential conflicts of interest.

AUTHOR CONTRIBUTIONS

- 548 Shan Cong: Conceptualization, Methodology, Software, Formal analysis, Validation, Writing - Original
- 549 Draft. Xiaohui Yao: Formal analysis, Validation, Writing - Review & Editing. Jingwen Yan: Data
- 550 Curation, Resources Writing - Review & Editing. Linhui Xie: Data Curation, Software, Writing - Review
- & Editing. Li Shen: Supervision, Conceptualization, Methodology, Writing Review & Editing. 551

FUNDING

- This work was supported in part by NIH R01 EB022574, R01 LM013463 and R21 AG066135, and by 552
- NSF 1837964, 1942394, and 1755836. 553

ACKNOWLEDGMENTS

- **ADNI Acknowledgements:** Data collection and sharing for this project was funded by the Alzheimer's
- Disease Neuroimaging Initiative (ADNI) (National Institutes of Health Grant U01 AG024904) and 555
- DOD ADNI (Department of Defense award number W81XWH-12-2-0012). ADNI is funded by the 556
- National Institute on Aging, the National Institute of Biomedical Imaging and Bioengineering, and through 557
- 558 generous contributions from the following: AbbVie, Alzheimer's Association; Alzheimer's Drug Discovery
- 559 Foundation; Araclon Biotech; BioClinica, Inc.; Biogen; Bristol-Myers Squibb Company; CereSpir, Inc.;
- Cogstate; Eisai Inc.; Elan Pharmaceuticals, Inc.; Eli Lilly and Company; EuroImmun; F. Hoffmann-La 560
- Roche Ltd and its affiliated company Genentech, Inc.; Fujirebio; GE Healthcare; IXICO Ltd.; Janssen 561
- Alzheimer Immunotherapy Research & Development, LLC.; Johnson & Johnson Pharmaceutical Research 562
- & Development LLC.; Lumosity; Lundbeck; Merck & Co., Inc.; Meso Scale Diagnostics, LLC.; NeuroRx 563

- Research; Neurotrack Technologies; Novartis Pharmaceuticals Corporation; Pfizer Inc.; Piramal Imaging;
- 565 Servier; Takeda Pharmaceutical Company; and Transition Therapeutics. The Canadian Institutes of Health
- 566 Research is providing funds to support ADNI clinical sites in Canada. Private sector contributions are
- 567 facilitated by the Foundation for the National Institutes of Health (www.fnih.org). The grantee organization
- 568 is the Northern California Institute for Research and Education, and the study is coordinated by the
- 569 Alzheimer's Therapeutic Research Institute at the University of Southern California. ADNI data are
- 570 disseminated by the Laboratory for Neuro Imaging at the University of Southern California.
- 571 HCP Acknowledgements: Data were provided by the Human Connectome Project, WU-Minn
- 572 Consortium (Principal Investigators: David Van Essen and Kamil Ugurbil; 1U54MH09-1657) funded by
- 573 the 16 NIH Institutes and Centers that support the NIH Blueprint for Neuroscience Research; and by the
- 574 McDonnell Center for Systems Neuroscience at Washington University.

DATA AVAILABILITY STATEMENT

- 575 The datasets ANALYZED for this study can be found in the ADNI (http://adni.loni.usc.edu/) and HCP
- 576 (https://www.humanconnectome.org/).

REFERENCES

- 577 Alloza, C., Cox, S. R., Cábez, M. B., Redmond, P., Whalley, H., Ritchie, S., et al. (2018). Polygenic risk
- score for schizophrenia and structural brain connectivity in older age: A longitudinal connectome and
- tractography study. Neuroimage 183, 884–896
- 580 Azevedo, E. P., Pomeranz, L., Cheng, J., Schneeberger, M., Vaughan, R., Stern, S. A., et al. (2019). A role
- of drd2 hippocampal neurons in context-dependent food intake. Neuron 102, 873–886
- Baron, R. M. and Kenny, D. A. (1986). The moderator-mediator variable distinction in social psychological
- research: Conceptual, strategic, and statistical considerations. *Journal of personality and social*
- 584 *psychology* 51, 1173
- 585 Bell, R. P., Barnes, L. L., Towe, S. L., Chen, N.-k., Song, A. W., and Meade, C. S. (2018). Structural
- connectome differences in hiv infection: brain network segregation associated with nadir cd4 cell count.
- 587 *Journal of neurovirology* 24, 454–463
- 588 Bertolero, M. A., Blevins, A. S., Baum, G. L., Gur, R. C., Gur, R. E., Roalf, D. R., et al. (2019). The network
- architecture of the human brain is modularly encoded in the genome. *arXiv preprint arXiv:1905.07606*
- 590 Burzynska, A. Z., Preuschhof, C., Bäckman, L., Nyberg, L., Li, S.-C., Lindenberger, U., et al. (2010). Age-
- related differences in white matter microstructure: region-specific patterns of diffusivity. *Neuroimage* 49,
- 592 2104–2112
- 593 Cauda, F., Nani, A., Manuello, J., Premi, E., Palermo, S., Tatu, K., et al. (2018). Brain structural alterations
- are distributed following functional, anatomic and genetic connectivity. *Brain* 141, 3211–3232
- 595 Chen, V. C.-H., Liu, Y.-C., Chao, S.-H., McIntyre, R. S., Cha, D. S., Lee, Y., et al. (2018). Brain structural
- networks and connectomes: the brain–obesity interface and its impact on mental health. *Neuropsychiatric*
- 597 disease and treatment 14, 3199
- 598 Cohen, J. R. and D'Esposito, M. (2016). The segregation and integration of distinct brain networks and
- their relationship to cognition. *Journal of Neuroscience* 36, 12083–12094
- 600 Cong, S., Risacher, S. L., West, J. D., Wu, Y.-C., Apostolova, L. G., Tallman, E., et al. (2018). Volumetric
- comparison of hippocampal subfields extracted from 4-minute accelerated vs. 8-minute high-resolution
- 602 t2-weighted 3t mri scans. Brain imaging and behavior 12, 1583–1595

- 603 Cong, S., Yao, X., Huang, Z., Risacher, S. L., Nho, K., Saykin, A. J., et al. (2020). Volumetric gwas of
- medial temporal lobe structures identifies an erc1 locus using adni high-resolution t2-weighted mri data.
- 605 Neurobiology of Aging
- 606 Cook, P., Bai, Y., Nedjati-Gilani, S., Seunarine, K., Hall, M., Parker, G., et al. (2006). Camino: open-source
- diffusion-mri reconstruction and processing. In 14th scientific meeting of the international society for
- 608 magnetic resonance in medicine (Seattle WA, USA), vol. 2759, 2759
- 609 Elliott, L. T., Sharp, K., Alfaro-Almagro, F., Shi, S., Miller, K. L., Douaud, G., et al. (2018). Genome-wide
- association studies of brain imaging phenotypes in uk biobank. *Nature* 562, 210–216
- 611 Elsheikh, S. S., Chimusa, E. R., Mulder, N. J., and Crimi, A. (2020). Genome-wide association study of
- brain connectivity changes for alzheimer's disease. Scientific Reports 10, 1–16
- 613 Emmerzaal, T. L., Kiliaan, A. J., and Gustafson, D. R. (2015). 2003-2013: a decade of body mass index,
- alzheimer's disease, and dementia. *Journal of Alzheimer's Disease* 43, 739–755
- 615 Gao, C. (2017). Investigation of the genetic architecture of cardiometabolic disease. Ph.D. thesis, Wake
- Forest University, 1834 Wake Forest Rd, Winston-Salem, NC 27109
- 617 Gao, C., Wang, N., Guo, X., Ziegler, J. T., Taylor, K. D., Xiang, A. H., et al. (2015). A comprehensive
- analysis of common and rare variants to identify adiposity loci in hispanic americans: the iras family
- 619 study (irasfs). *PloS one* 10
- 620 Gómez-Ambrosi, J., Catalán, V., Diez-Caballero, A., Martínez-Cruz, L. A., Gil, M. J., García-Foncillas, J.,
- et al. (2004). Gene expression profile of omental adipose tissue in human obesity. *The FASEB journal*
- 622 18, 215–217
- 623 Gómez-Apo, E., García-Sierra, A., Silva-Pereyra, J., Soto-Abraham, V., Mondragón-Maya, A., Velasco-
- Vales, V., et al. (2018). A postmortem study of frontal and temporal gyri thickness and cell number in
- 625 human obesity. *Obesity* 26, 94–102
- 626 Gong, G., He, Y., and Evans, A. C. (2011). Brain connectivity: gender makes a difference. The
- 627 *Neuroscientist* 17, 575–591
- 628 Guo, Y., Shen, X.-N., Hou, X.-H., Ou, Y.-N., Huang, Y.-Y., Dong, Q., et al. (2020). Genome
- wide association study of white matter hyperintensity volume in elderly persons without dementia.
- 630 NeuroImage: Clinical 26, 102209
- 631 Hair, B. (2014). Body Mass Index, Breast Tissue, and the Epigenome. Ph.D. thesis, University of North
- 632 Carolina at Chapel Hill
- 633 Imai, K., Keele, L., and Tingley, D. (2010). A general approach to causal mediation analysis. *Psychol*
- 634 *Methods* 15, 309–334
- 635 Jahanshad, N., Rajagopalan, P., Hua, X., Hibar, D. P., Nir, T. M., Toga, A. W., et al. (2013). Genome-
- wide scan of healthy human connectome discovers spon1 gene variant influencing dementia severity.
- 637 Proceedings of the National Academy of Sciences 110, 4768–4773
- 638 Jiang, X., Shen, Y., Yao, J., Zhang, L., Xu, L., Feng, R., et al. (2019). Connectome analysis of functional
- and structural hemispheric brain networks in major depressive disorder. Translational psychiatry 9,
- 640 1–12
- 641 Jørstad, K. E. and Næevdal, G. (1996). Breeding and genetics. Developments in Aquaculture and Fisheries
- 642 *Science* 29, 655–725
- 643 Karwowski, W., Vasheghani Farahani, F., and Lighthall, N. (2019). Application of graph theory for
- identifying connectivity patterns in human brain networks: a systematic review. Frontiers in Neuroscience
- 645 13, 585

- 646 Keown, C. L., Datko, M. C., Chen, C. P., Maximo, J. O., Jahedi, A., and Müller, R.-A. (2017). Network
- organization is globally atypical in autism: a graph theory study of intrinsic functional connectivity.
- 648 Biological Psychiatry: Cognitive Neuroscience and Neuroimaging 2, 66–75
- 649 Kochunov, P., Glahn, D. C., Lancaster, J. L., Winkler, A. M., Smith, S., Thompson, P. M., et al. (2010).
- 650 Genetics of microstructure of cerebral white matter using diffusion tensor imaging. *Neuroimage* 53,
- 651 1109–1116
- 652 Kochunov, P., Jahanshad, N., Marcus, D., Winkler, A., Sprooten, E., Nichols, T. E., et al. (2015).
- Heritability of fractional anisotropy in human white matter: a comparison of human connectome project
- and enigma-dti data. *Neuroimage* 111, 300–311
- 655 Latora, V. and Marchiori, M. (2001). Efficient behavior of small-world networks. Physical review letters
- 656 87, 198701
- 657 Li, L., Wang, X., Liu, X., Guo, R., and Zhang, R. (2019). Integrative analysis reveals key mrnas and
- lncrnas in monocytes of osteoporotic patients. Mathematical biosciences and engineering: MBE 16,
- 659 5947–5971
- 660 Lopez-Larson, M. P., Anderson, J. S., Ferguson, M. A., and Yurgelun-Todd, D. (2011). Local brain
- 661 connectivity and associations with gender and age. Developmental cognitive neuroscience 1, 187–197
- Lowe, C. J., Reichelt, A. C., and Hall, P. A. (2019). The prefrontal cortex and obesity: a health neuroscience
- perspective. *Trends in cognitive sciences* 23, 349–361
- 664 Mak, E., Colloby, S. J., Thomas, A., and O'Brien, J. T. (2016). The segregated connectome of late-life
- depression: a combined cortical thickness and structural covariance analysis. Neurobiology of aging 48,
- 666 212–221
- Mohr, H., Wolfensteller, U., Betzel, R. F., Mišić, B., Sporns, O., Richiardi, J., et al. (2016). Integration and
- segregation of large-scale brain networks during short-term task automatization. *Nature communications*
- 669 7, 1–12
- 670 Mrozikiewicz, A. E., Bogacz, A., Barlik, M., Górska, A., Wolek, M., and Kalak, M. (2019). The role of
- folate receptor and reduced folate carrier polymorphisms in osteoporosis development. *Herba Polonica*
- 672 65, 30–36
- Newman, M. E. (2003). The structure and function of complex networks. SIAM review 45, 167–256
- Newman, M. E. (2006). Modularity and community structure in networks. *Proceedings of the national*
- 675 *academy of sciences* 103, 8577–8582
- 676 Onnela, J.-P., Saramäki, J., Kertész, J., and Kaski, K. (2005). Intensity and coherence of motifs in weighted
- 677 complex networks. *Physical Review E* 71, 065103
- 678 Ou, X., Andres, A., Pivik, R., Cleves, M. A., and Badger, T. M. (2015). Brain gray and white matter
- differences in healthy normal weight and obese children. Journal of Magnetic Resonance Imaging 42,
- 680 1205–1213
- Palmer, N. D., Goodarzi, M. O., Langefeld, C. D., Wang, N., Guo, X., Taylor, K. D., et al. (2015). Genetic
- variants associated with quantitative glucose homeostasis traits translate to type 2 diabetes in mexican
- americans: the guardian (genetics underlying diabetes in hispanics) consortium. *Diabetes* 64, 1853–1866
- Peven, J. C., Litz, G. A., Brown, B., Xie, X., Grove, G. A., Watt, J. C., et al. (2019). Higher cardiorespiratory
- 685 fitness is associated with reduced functional brain connectivity during performance of the stroop task.
- 686 Brain Plasticity, 1–11
- 687 Purcell, S., Neale, B., Todd-Brown, K., Thomas, L., Ferreira, M. A., Bender, D., et al. (2007). Plink: a
- tool set for whole-genome association and population-based linkage analyses. *The American journal of*
- 689 *human genetics* 81, 559–575

- 690 Rapuano, K. M., Huckins, J. F., Sargent, J. D., Heatherton, T. F., and Kelley, W. M. (2016). Individual
- differences in reward and somatosensory-motor brain regions correlate with adiposity in adolescents.
- 692 *Cerebral cortex* 26, 2602–2611
- Rubinov, M. and Sporns, O. (2010). Complex network measures of brain connectivity: uses and interpretations. *Neuroimage* 52, 1059–1069
- Rudie, J. D., Brown, J., Beck-Pancer, D., Hernandez, L., Dennis, E., Thompson, P., et al. (2013). Altered
- functional and structural brain network organization in autism. *NeuroImage: clinical* 2, 79–94
- 697 Sala-Llonch, R., Bartrés-Faz, D., and Junqué, C. (2015). Reorganization of brain networks in aging: a
- review of functional connectivity studies. Frontiers in psychology 6, 663
- 699 Salzwedel, A. P., Gao, W., Andres, A., Badger, T. M., Glasier, C. M., Ramakrishnaiah, R. H., et al. (2019).
- Maternal adiposity influences neonatal brain functional connectivity. *Frontiers in human neuroscience* 12, 514
- 702 Saykin, A. J., Shen, L., Foroud, T. M., Potkin, S. G., Swaminathan, S., Kim, S., et al. (2010). Alzheimer's
- disease neuroimaging initiative biomarkers as quantitative phenotypes: Genetics core aims, progress,
- and plans. Alzheimer's & dementia 6, 265–273
- 705 Saykin, A. J., Shen, L., Yao, X., Kim, S., Nho, K., Risacher, S. L., et al. (2015). Genetic studies of
- quantitative mci and ad phenotypes in adni: Progress, opportunities, and plans. Alzheimer's & Dementia
- 707 11, 792–814
- 708 Shen, L. and Thompson, P. M. (2020). Brain imaging genomics: Integrated analysis and machine learning.
- 709 *Proceedings of the IEEE* 108, 125–162
- 710 Shu, N., Liu, Y., Duan, Y., and Li, K. (2015). Hemispheric asymmetry of human brain anatomical network
- revealed by diffusion tensor tractography. *BioMed research international* 2015
- 712 Smith, R. E., Tournier, J.-D., Calamante, F., and Connelly, A. (2015). Sift2: Enabling dense quantitative
- assessment of brain white matter connectivity using streamlines tractography. *Neuroimage* 119, 338–351
- 714 Sporns, O. (2013). Network attributes for segregation and integration in the human brain. Current Opinion
- 715 *in Neurobiology* 23, 162–171
- 716 Stenholm, S., Head, J., Aalto, V., Kivimäki, M., Kawachi, I., Zins, M., et al. (2017). Body mass index
- as a predictor of healthy and disease-free life expectancy between ages 50 and 75: a multicohort study.
- 718 International journal of obesity 41, 769–775
- 719 Sun, Y., Chen, Y., Collinson, S. L., Bezerianos, A., and Sim, K. (2017). Reduced hemispheric asymmetry
- of brain anatomical networks is linked to schizophrenia: a connectome study. *Cerebral Cortex* 27,
- 721 602–615
- 722 Thompson, P. M., Ge, T., Glahn, D. C., Jahanshad, N., and Nichols, T. E. (2013). Genetics of the
- 723 connectome. *Neuroimage* 80, 475–488
- 724 Tian, L., Wang, J., Yan, C., and He, Y. (2011). Hemisphere-and gender-related differences in small-world
- brain networks: a resting-state functional mri study. *Neuroimage* 54, 191–202
- 726 Tournier, J.-D., Calamante, F., and Connelly, A. (2012). Mrtrix: diffusion tractography in crossing fiber
- regions. *International journal of imaging systems and technology* 22, 53–66
- 728 Tzourio-Mazoyer, N., Landeau, B., Papathanassiou, D., Crivello, F., Etard, O., Delcroix, N., et al. (2002).
- Automated anatomical labeling of activations in spm using a macroscopic anatomical parcellation of the
- mni mri single-subject brain. *Neuroimage* 15, 273–289
- van den Heuvel, M. P., Scholtens, L. H., de Lange, S. C., Pijnenburg, R., Cahn, W., van Haren, N. E., et al.
- 732 (2019). Evolutionary modifications in human brain connectivity associated with schizophrenia. *Brain*
- 733 142, 3991–4002

- Van Essen, D. C., Smith, S. M., Barch, D. M., Behrens, T. E., Yacoub, E., Ugurbil, K., et al. (2013). The wu-minn human connectome project: an overview. *Neuroimage* 80, 62–79 735
- Varangis, E., Habeck, C., Razlighi, Q., and Stern, Y. (2019). The effect of aging on resting state connectivity 736 of predefined networks in the brain. Frontiers in aging neuroscience 11, 234 737
- Veit, R., Kullmann, S., Heni, M., Machann, J., Häring, H.-U., Fritsche, A., et al. (2014). Reduced cortical 738 thickness associated with visceral fat and bmi. NeuroImage: Clinical 6, 307–311 739
- Xie, L., Amico, E., Salama, P., Wu, Y.-c., Fang, S., Sporns, O., et al. (2018). Heritability estimation of 740
- reliable connectomic features. In International Workshop on Connectomics in Neuroimaging (Springer), 741
- 742 58-66
- Yan, J., Liu, K., Lv, H., Amico, E., Risacher, S. L., Wu, Y.-c., et al. (2018). Joint exploration and mining of 743
- memory-relevant brain anatomic and connectomic patterns via a three-way association model. In 2018 744
- IEEE 15th International Symposium on Biomedical Imaging (ISBI 2018) (IEEE), 6–9 745
- Yao, X., Cong, S., Yan, J., Risacher, S. L., Saykin, A. J., Moore, J. H., et al. (2020). Regional imaging 746 genetic enrichment analysis. Bioinformatics 36, 2554–2560 747
- Yao, X., Risacher, S. L., Nho, K., Saykin, A. J., Wang, Z., Shen, L., et al. (2019). Targeted genetic analysis 748
- of cerebral blood flow imaging phenotypes implicates the inpp5d gene. Neurobiology of Aging 81, 749
- 213-221 750
- Yokum, S., Ng, J., and Stice, E. (2012). Relation of regional gray and white matter volumes to current bmi 751
- and future increases in bmi: a prospective mri study. International Journal of Obesity 36, 656-664 752
- Zhao, T., Cao, M., Niu, H., Zuo, X.-N., Evans, A., He, Y., et al. (2015). Age-related changes in the 753
- topological organization of the white matter structural connectome across the human lifespan. Human 754 brain mapping 36, 3777–3792
- 755
- Zhong, S., He, Y., Shu, H., and Gong, G. (2017). Developmental changes in topological asymmetry 756
- between hemispheric brain white matter networks from adolescence to young adulthood. Cerebral 757
- Cortex 27, 2560–2570 758
- Zuo, X.-N., Ehmke, R., Mennes, M., Imperati, D., Castellanos, F. X., Sporns, O., et al. (2012). Network 759
- centrality in the human functional connectome. Cerebral cortex 22, 1862–1875 760

TABLES

Table 1. Participant characteristics in HCP and ADNI genetic association analyses.

Cohort	НСР	ADNI	P	
Number	275	178	-	
Gender(M/F)	137/138	108/70	3.02E-02	
Age	28.69 ± 3.64	73.76 ± 6.95	5.56E-175	
Education	15.14 ± 1.64	16.03 ± 2.78	1.41E-04	
MMSE	29.09 ± 1.04	27.37 ± 2.54	2.28E-15	
Weight	77.70 ± 17.06	77.71 ± 15.92	1.00	
BMI	25.99 ± 4.73	27.28 ± 5.24	8.87E-03	
clus coef ROI 087	0.51 ± 0.05	0.29 ± 0.13	1.41E-55	
loc effi ROI 087	0.52 ± 0.05	0.39 ± 0.17	1.20E-18	

P-values were assessed because of significant differences among diagnosis groups, and were computed using one-way ANOVA (except for gender using χ^2 test). The p values < 0.05 are shown in bold. HC = Healthy Control; EMCI = Early Mild Cognitive Complaint; LMCI = Late Mild Cognitive Complaint; AD = Alzheimer's Disease

	ADNI	\mathbf{p}^c	1.65E-01	2.15E-01	2.15E-01	1.98E-01	4.71E-01	5.68E-01	ı	1.63E-03	ı	3.51E-01	2.02E-01	2.02E-01	1.33E-01	1.62E-01	4.82E-01	5.71E-01	ı	1.34E-03	ı	1
	1	Beta	-0.10	0.09	0.09	-0.10	-0.05	-0.04	ı	-3.20	ı	-0.07	0.10	0.10	-0.11	-0.11	-0.05	-0.04	ı	-0.24	ı	
sohorts.	HCP	Ь	1.25E-10	8.00E-12	7.52E-12	7.71E-11	1.51E-10	8.26E-12	7.16E-11	1.09E-10	5.54E-12	4.68E-11	7.75E-12	7.36E-12	1.56E-10	1.86E-11	6.84E-11	3.71E-12	5.98E-11	4.22E-11	1.74E-11	2.72E-10
ADNI 6		Beta	-0.36	-0.39	-0.39	-0.37	-0.37	-0.39	-0.38	-0.37	-0.40	-0.38	-0.39	-0.39	-0.37	-0.38	-0.38	-0.40	-0.38	-0.38	-0.39	-0.37
statistics in the HCP and	Clocast ganab	Closest gene	1	TMEM200C	TMEM200C	AKR1C4			DEFB134/DEFB135/ DEFB136	ANAPC15/LRTOMT/ FOLR3/LAMTOR1	ST14	-	TMEM200C	TMEM200C	AKR1C4	AKR1C4		- (DEFB134/DEFB135/ DEFB136	ANAPC15/LRTOMT/ FOLR3/LAMTOR1	ST14	1
on measures:	B D <i>a</i>	10	148788006	5927441	5930979	5273767	66436114	66485112	11859985	71841325	130043580	148788006	5927441	5930979	5273767	5273767	66436114	66485112	11859985	71841325	130043580	29291173
s and segregation	SNP		rs6930337	rs1940608	rs4798416	rs2104994	rs9994092	rs10032124	rs4841664	rs7937515	rs1461192	rs6930337	rs1940608	rs4798416	rs2104994	rs2104994	rs9994092	rs10032124	rs4841664	rs7937515	rs1461192	rs147446959
een SNF	CHR	1	9	18	18	10	4	4	~	11	11	9	18	18	10	10	4	4	~	11	11	21
iations betwe	ROI			FMidO_R FMedO_R TPMid_L							FMidO_R FMedO_L FMedO_R TPMid_L											
Table 2. Significant associations between SNPs and segregation measures: statistics in the HCP and ADNI cohorts	Segregation measure	oegieganon measure	Clustering coefficient													Local efficiency						

Table 2. Note: a Build 37, assembly hg19. b Genes located ±100 kb of the top SNP. c P value reaching the Bonferroni corrected threshold (0.05/20=2.25E-03) is shown in bold. Abbreviations: F = frontal, TP = temporal pole, Mid = middle, Med = medial, Orb = orbital, L = left, R =

Table 3. Associations between rs7937515 and brain network measures.

Class	QT	ROI or	HCP		ADNI		
Class	Q1	Global	Beta	P	Beta	P	
Segregation	Clustering coefficient	TPMid_L	-0.37	1.09E-10	-0.24	1.63E-03	
	Clustering coefficient	TPMid_R	-0.20	3.53E-04	-0.22	3.94E-03	
	Local efficiency	TPMid_L	-0.38	4.22E-11	-0.24	1.34E-03	
	Local efficiency	TPMid_R	-0.22	7.05E-05	-0.22	2.92E-03	
	Transitivity	Global	-0.23	3.65E-05	-0.24	1.17E-03	
	Modularity	Global	0.20	5.32E-04	-0.12	9.32E-02	
Integration	Global efficiency	Global	-0.29	1.63E-07	-0.24	1.48E-03	
	Density	Global	-0.26	2.64E-06	0.03	7.11E-01	
Centrality	Betweenness centrality	TPMid_L	-0.09	1.28E-01	-0.05	5.28E-01	
	Betweenness centrality	TPMid_R	-0.06	3.24E-01	-0.03	6.75E-01	
	Eigenvector centrality	TPMid_L	-0.32	9.58E-08	-0.13	7.85E-02	
	Eigenvector centrality	TPMid_R	-0.20	6.11E-04	-0.03	6.98E-01	
Resilience	Assortativity coefficient	Global	0.10	1.14E-01	0.06	3.95E-01	

Table 3. Abbreviations: F = frontal, TP = temporal pole, Mid = middle, Med = medial, Orb = orbital, L = left, R = right, QT = quantitative trait.

FIGURE CAPTIONS

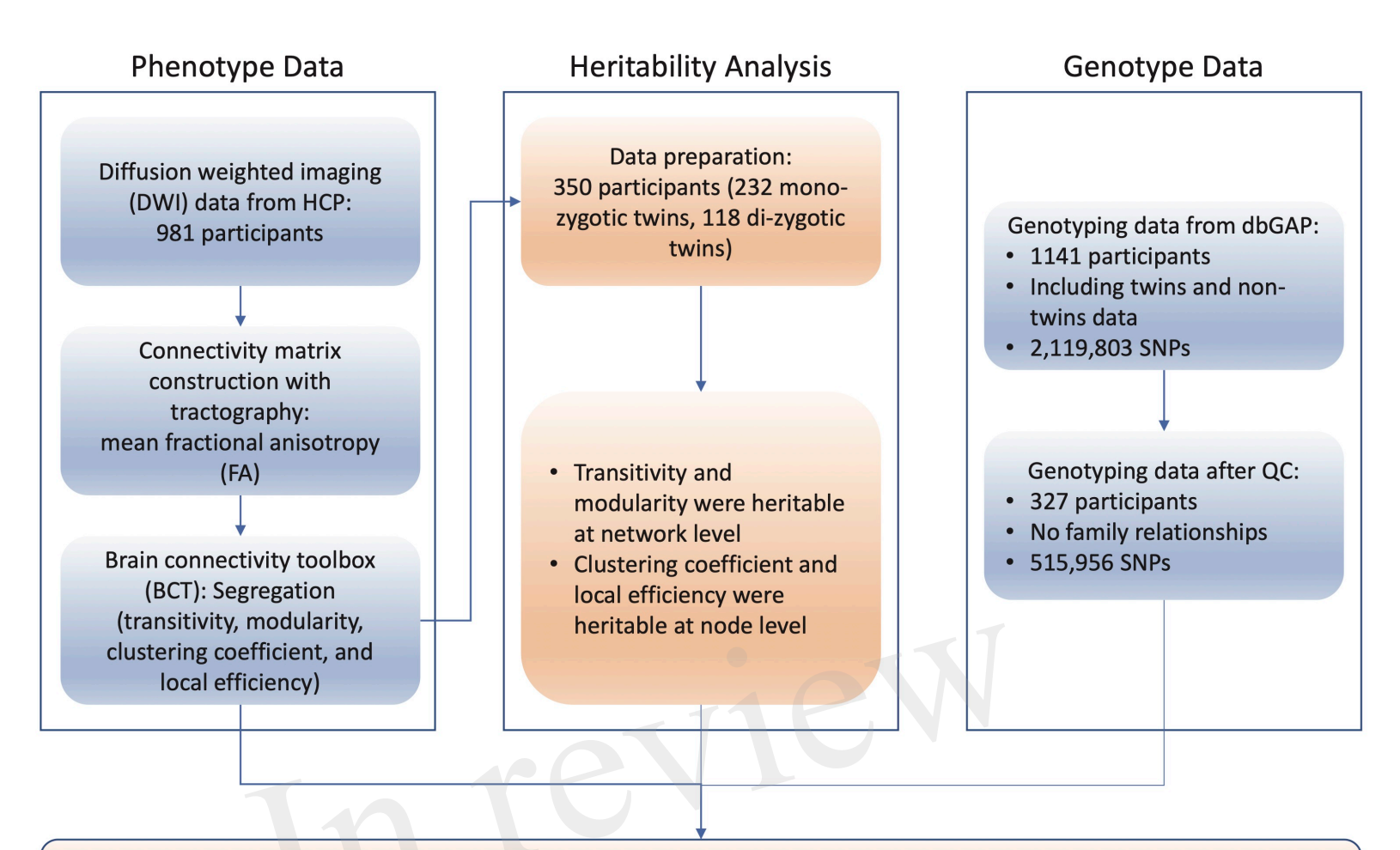
Figure 1. Flowchart of brain connectome GWAS design. Abbreviations: SNPs, single nucleotide polymorphisms; ADNI, Alzheimer's Disease Neuroimaging Initiative; HCP, Human Connectome Project; dbGaP, database of Genotypes and Phenotypes; QC, quality control; ROI, region of interest; iQT: imaging quantitative trait; BMI, body mass index.

Figure 2. Manhattan plot of GWAS results in the HCP dataset. Top and bottom plots show the GWAS results of clustering coefficient and local efficiency on left middle temporal gyrus, respectively. Red and blue lines correspond to the p-value of 5E-08 and 2.75E-10, respectively.

Figure 3. Association of rs7937515 on clustering coefficient and local efficiency of the left middle temporal gyrus. (A-B) Mean clustering coefficient with standard errors are plotted against the rs7937515 genotype groups (i.e., AA, AG and GG) for the HCP and ADNI cohorts, respectively. (C-D) Mean local efficiency with standard errors are plotted against the rs7937515 genotype groups (i.e., AA, AG and GG) for the HCP and ADNI cohorts, respectively. p values are calculated from GWAS (HCP) and targeted analysis (ADNI), and significant p values are marked in bold.

Figure 4. Association of rs7937515 on BMI in the HCP and ADNI cohorts. (A) Mean BMI with standard errors are plotted against the rs7937515 genotype groups (i.e., AA, AG and GG) for the HCP cohort. (B) Mean BMI with standard errors are plotted against the rs7937515 genotype groups (i.e., AA, AG and GG) for the ADNI cohort. p values are calculated from mediation analysis, and significant p values are marked in bold.

Figure 5. Direct and mediation effect of rs7937515 on BMI through left middle temporal gyrus. (A-B) illustrate the effect size, 95% CI and p value from rs7937515 mediation analysis of BMI via left middle temporal clustering coefficient. (C-D) illustrate the effect size, 95% confidence interval and p value from rs7937515 mediation analysis of BMI via left middle temporal local efficient. TE = total effect; DE = direct effect; ME = mediation effect.



Genome-wide association analysis (GWAS) of segregation measures (N = 275, 137 male, 138 female, age 28.69 ± 3.64) Several associations between ROI-measure ~ SNP were identified (corrected p threshold = 2.75E-10)

Targeted analysis of segregation phenotype from ADNI (N = 178, 108 male, 70 female, age 73.76 ± 6.95) Common associations were identified across HCP and ADNI datasets (corrected p threshold = 3.3E-03):

rs7937515 ~ clustering coefficient measured at left middle temporal gyrus

rs7937515 ~ local efficiency measured at left middle temporal gyrus

Mediation analysis for pathway of SNP rs7937515 ~ segregation measures (iQT) ~ common phenotypic outcome in both datasets:

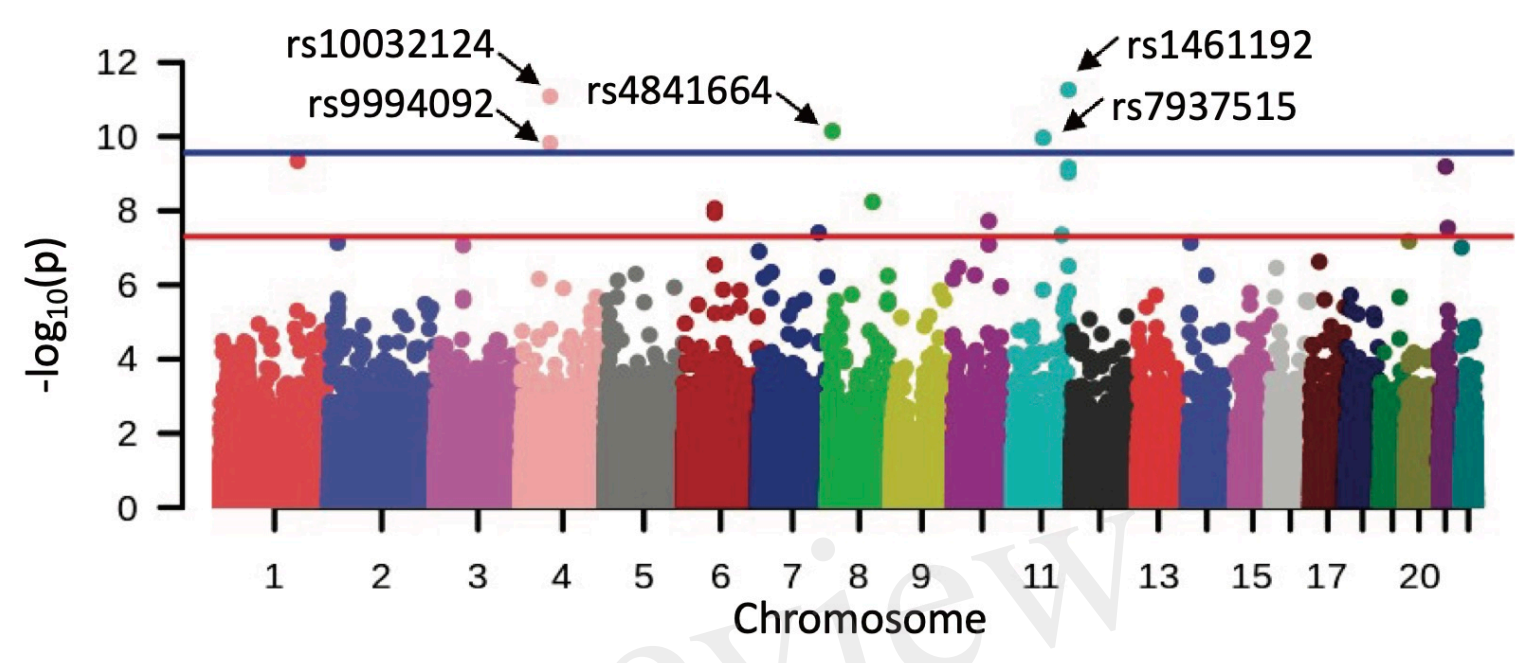
- HCP: BMI was influenced by rs7937515 with clustering coefficient and local efficiency as mediators
- ADNI: no such mediation effect was identified.

Targeted analysis of network segregation measures (iQT) and phenotypic outcome:

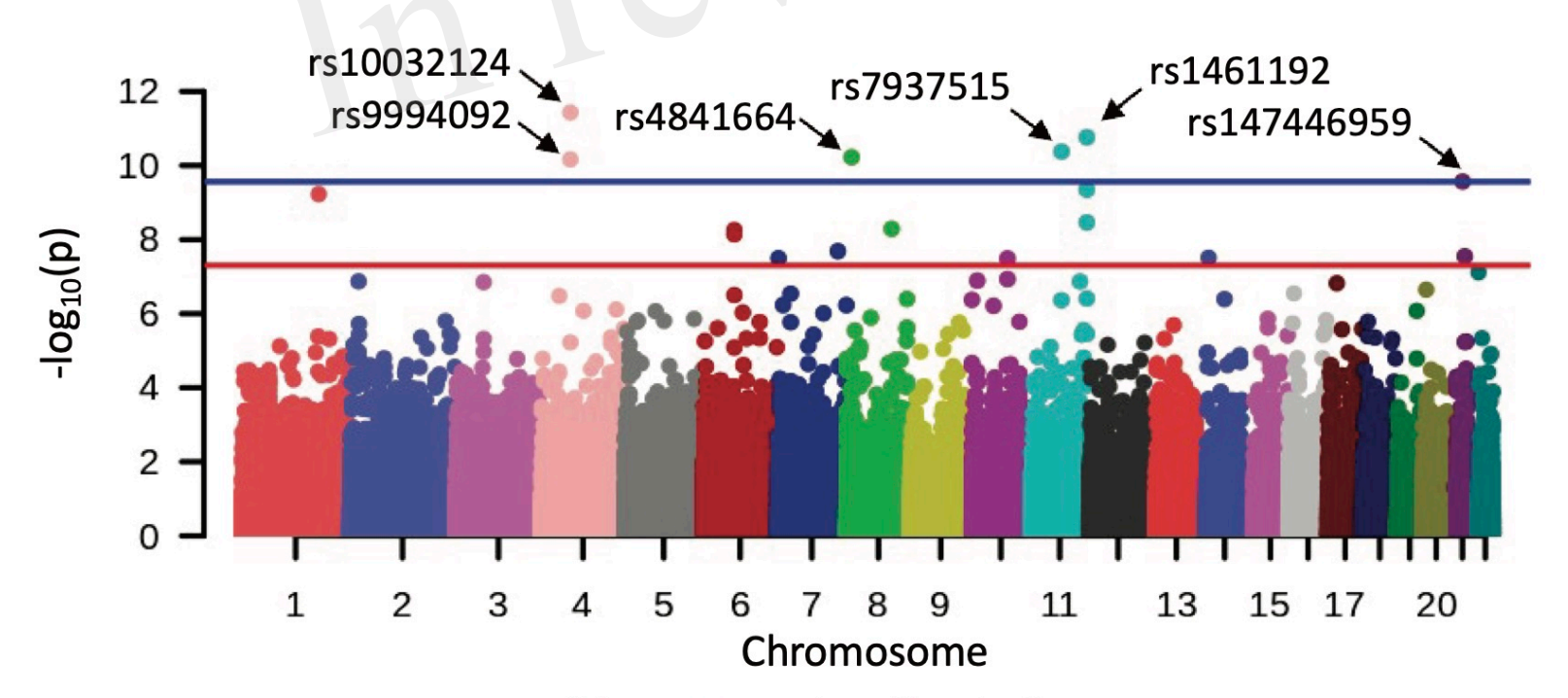
- HCP: clustering coefficient and local efficiency measured at left middle temporal gyrus were associated with BMI
- ADNI: no such association was identified

<u>Targeted analysis of SNP</u> <u>rs7937515</u> and other important <u>connectivity attributes (iQT):</u>

- HCP: rs7937515 associated with global efficiency, eigen centrality, assortativity, density, number of edge, and strength
- ADNI: rs7937515 associated with global efficiency, transitivity, and strength



(a) GWAS results of clustering coefficient.



(b) GWAS results of local efficiency.

